polysaccharides

MDPI

Article

Hydrogen Bond Integration in Potato Microstructure: Effects of Water Removal, Thermal Treatment, and Cooking Techniques

Iman Dankar [1], Amira Haddarah [2], Montserrat Pujolà [3] and Francesc Sepulcre [3,4,*]

[1] Department of Liberal Arts, Faculty of Arts and Sciences, Lebanese American University, Byblos P.O. Box 36, Lebanon; imandankar03@gmail.com
[2] Doctoral School of Science and Technology, EDST, Lebanese University, Hadath P.O. Box 14, Lebanon; amira.haddarah@ul.edu.lb
[3] Departament d'Enginyeria Agroalimentària i Biotecnologia, Universitat Politècnica de Catalunya, BarcelonaTECH, 08034 Barcelona, Spain; montserrat.pujola@upc.edu
[4] Centre de Biotecnologia Molecular, 08222 Terrassa, Spain
* Correspondence: francesc.sepulcre@upc.edu

Abstract: Fourier-transform infrared spectroscopy (FTIR), X-ray diffraction (XRD), and Scanning electron microscopy (SEM) were used to study the effects of heat treatments and water removal by freeze-drying after different time intervals (6, 12, 24, 48, and 72 h) on the molecular structure of potato tubers. SEM images show structural differences between raw (RP), microwaved (MP), and boiled potato (BP). MP showed a cracked structure. BP was able to re-associate into a granule-like structure after 6 h of freeze-dying, whereas RP had dried granules within a porous matrix after 24 h of freeze-drying. These results are consistent with the moisture content and FTIR results for MP and BP, which demonstrated dried spectra after 6 h of freeze-drying and relatively coincided with RP results after 24 h of freeze-drying. Additionally, three types of hydrogen bonds have been characterized between water and starch, and the prevalence of water very weakly bound to starch has also been detected. The relative crystallinity (RC) was increased by thermal treatment, whereby microwaving recorded the highest value. A comparison of the FTIR and XRD results indicated that freeze-drying treatment overcomes heat effects to generate an integral starch molecule.

Keywords: microwaved potato; boiled potato; raw potato; starch freeze-drying; lyophilization

Citation: Dankar, I.; Haddarah, A.; Pujolà, M.; Sepulcre, F. Hydrogen Bond Integration in Potato Microstructure: Effects of Water Removal, Thermal Treatment, and Cooking Techniques. *Polysaccharides* **2024**, *5*, 609–629. https://doi.org/10.3390/polysaccharides5040039

Academic Editor: Lesław Juszczak

Received: 23 May 2024
Revised: 9 July 2024
Accepted: 30 September 2024
Published: 11 October 2024

1. Introduction

Potatoes are the topmost-grown tubers and rank third in global crop production, following maize and wheat [1]. When freshly harvested, potatoes contain about 200 g kg^{-1} of dry matter, with starch being the main component. The raw starch in potato tubers is typically arranged into a void that houses granules of two kinds of α-glucans: amylopectin and amylose. Amylopectin is a highly branched α-glucan polymer with a high average molecular weight, consisting of an α (1 → 4)-linked backbone and α (1 → 6)-linked branches of α-glucosidic bonds. On the other hand, amylose is a linear and comparatively long α-glucan polymer connected by α (1 → 4)-linkages. The raw starch granules exhibit a crystalline/amorphous structure that can be identified at both short (nm) and long (several μm) scales [2]. This defined molecular structure provides starch with malleable characteristics and wide applications in the food industry such as gelling, thickening, or encapsulating agents. However, to meet specific end requirements, starches are usually modified by physical and chemical treatments [3].

To this end, potato tubers are commonly cooked before consumption using various methods, such as boiling, frying, baking, or microwaving, which produce potatoes with different mechanical, sensorial, and nutrient bioavailability characteristics according to the type of cooking method used [4]. Romano et al. [5] found that depending on the process type, the elasticity modulus of the cooked potatoes displayed the following order: baked

potatoes > boiled > fried potatoes. For instance, microwaving potatoes were reported to be heated comparatively faster in a homogenous manner, directing the dipole hydrogen bonds via high-energy electromagnetic radiation inducing a firmer texture than boiling and baking [6]. Moreover, individual sugar content was reported to increase during baking and microwaving compared to that during boiling [7]. The primary transformations that occur during cooking can be outlined as follows: the potato tissue softens due to heat, leading to a breakdown of cell membrane integrity; the bonds between intact cells weaken, causing them to separate and resulting in a loss of turgidity. Furthermore, cooking encourages starch expansion by altering the proportion of water available and triggering gelatinization [8–11].

In addition, variations in water availability contribute to the composition of expanded granules that occupy the intercellular space between amylose and the amylopectin network, subsequently influencing the texture of potatoes by enhancing starch rigidity [12,13]. The increased rigidity of the starch gel is accompanied by crystal formation, which is influenced by storage temperature and duration [14,15]. The internal microstructure of starch, which directly impacts its textural and organoleptic properties, is controlled by the applied temperature and the present water content [9,16].

Therefore, gaining a deeper understanding of starch flexibility at the microstructural level in response to external physical factors, such as water content and thermal energy, could be crucial in understanding the physio-mechanical and organoleptic changes induced in potatoes under varying storage conditions or cooking processes. The microstructural level of starch could be examined in the short-range order using FTIR (Fourier transform infrared spectroscopy) to detect the folding of amylose/amylopectin chains, the crystalline/amorphous ratio, or even the retro-gradation of potato starch [17–19]. In this context, the structure of the OH vibration band revealed by FTIR can provide information about the network of hydrogen bonds and their modifications (rearrangement, breakdown, etc.) due to different processing treatments. Three types of water have been suggested for potato starch: anisotropically bound water, trapped water, and a third type that is an average between free and weakly bound water populations. Interactions and H-exchange between water and OH-from the glucose ring have also been studied [20].

Though the water content and water distribution in starches have been studied and reported in several articles, no works about the extent of the distribution and strength of the hydrogen bonds formed by the water–starch interactions have been published yet. In general, in biological samples, water presents a broad band in the region between 3700–3100 cm^{-1}, usually centered at about 3400 cm^{-1} corresponding with the major two fundamental vibrational modes of isolate water molecules that are located at 3618 cm^{-1} (asymmetric stretching) and 3414 cm^{-1} (symmetric stretching), and another vibrational mode at 1650 cm^{-1} (flexion). This FTIR region between 3700 cm^{-1} and 3000 cm^{-1} has been used to study the distribution of the hydrogen bonds in different materials containing water [21].

Moreover, the microstructural level of starch can be examined in the long-range order using XRD (X-ray diffraction). This technique allows us to understand the structure of starch and identify any alterations in the crystalline pattern (such as starch aging, softening, or gelatinization) that may occur due to various processing methods [22]. A more thorough and evidence-based combination of data in both the short- and long-range orders (FTIR and XRD, respectively) can be achieved through the visual examination and characterization of the starch microstructure using SEM (scanning electron microscope). This tool provides a detailed visualization of starch molecules and their arrangement and offers a more definitive method for identifying and understanding differences between structures of different origins or with varying properties of processing.

This study aims to analyze and compare how external physical parameters, such as thermal exposure, cooking method (boiling, microwaving), and freeze-drying treatment/water availability, actively influence the structural changes in potato starch molecules, with a deeper evaluation of the sensitivity of starch–water hydrogen bond interactions to these external factors. Thus, allowing a broader understanding of the mechanical and

organoleptic properties of potatoes displayed during various processing treatments. For this, FTIR spectra, XRD patterns, and SEM images were collected for raw potato (RP), microwaved potato (MP), and boiled potato (BP) before (t = 0) and after freeze-drying at intervals of 6, 12, 24, 48, and 72 h. This was followed by a deep investigation of the hydrogen bonding strength at different physiological parameters using MATLAB.

2. Materials and Methods

2.1. Sample Preparation

Fresh potato tubers (*Solanum Tuberosum* L. cv. Kennebec) of approximately the same size acquired from a local supermarket were selected, washed thoroughly, and subjected to two different treatments: microwave heating and boiling. During microwave heating, a potato tuber was cooked at full power (700 W for 12 min). For boiling, a potato tuber was placed in a beaker filled with distilled water and left to boil for 25 min. Samples were then removed and, along with raw potato tubers (control), peeled and cut immediately into cubes (2 cm side) in preparation for further analysis.

2.2. Freeze Drying (Freeze-Drying)

Two lots of samples were frozen overnight at −80 °C and then dried using a CHRIST freeze drier (Alpha 1–4 LD plus, 15386, Osterode am Harz, Germany,) for 6, 12, 24, 48, and 72 h. After each time point, samples of the first lot were taken, ground, and examined by FTIR (Fourier Transform Infrared Spectroscopy, ThermoFisher Scientific; Madrid, Spain), XRD (X-ray Diffraction, Bruker D8 Discover (AXS GmbH, Berlin, Germany)), and SEM (Scanning Electron Microscopy, SERON SCI2100, Seron Technologies Inc., Uiwang-si, Republic of Korea). As for the second lot, samples were determined for their moisture content using hot air oven drying.

2.3. Moisture Content

The moisture content of the samples before and after the lyophilization stages was determined by the oven-drying method [23]. Samples were lyophilized for the respective time (6, 12, 24, 48, and 72 h), weighed, and then placed in an oven at 85 °C for 3 days. Samples examined without freeze-drying were immediately prepared, measured for their weight, and placed in the oven. Final weights after oven drying were measured and moisture content was calculated according to the following equation:

$$\text{MC (\%)} = (\text{W} - \text{D})/\text{W} \times 100$$

where MC is the moisture content (%), W is the initial weight before oven drying (g), and D is the weight of the sample after oven drying (g). The results are represented as an average value of 3 measurements.

2.4. Fourier Transform Infrared Spectroscopy (FTIR)

FTIR spectra were collected for potato cubes prepared using different cooking methods (microwaved and boiled) as well as raw potato cubes at time 0 (initially before freeze-drying) and after being freeze-dried for 6, 12, 24, 48, and 72 h on an STS FTIR spectrometer (ThermoFisher Scientific; Madrid, Spain). Spectra were recorded in the range of wavenumber 349 to 4000 cm^{-1} by an MCT detector cooled with liquid nitrogen. Then, 200 mg of dried KBr was weighed using an analytical balance. A small amount (2 mg) of the dried starch sample was added, blended with KBr, and pressed into tablets before measurements. The ratio of sample to KBr should be around 1–2% to ensure good dispersion and transparency in the IR spectrum. Spectra were collected at a resolution of 4 cm^{-1} and an average of 35 numbers of scans per sample.

2.5. Curve-Fitting Analysis

Curve fitting for the peak deconvolution was performed by MATLAB R2023a, Update 2 (9.14.0.2254940). Shape bands were assumed to be Gaussian because these bands have been previously used to fit the OH vibrational spectra and best describe the thermally broadened states (Schmidt and Miki, 2007 [24]). Although different numbers of bands from 2 to 5 have been tested for all the samples, the best fits have been achieved by considering three Gaussian bands, initially centered around 3618 cm^{-1}, 3414 cm^{-1}, and 3180 cm^{-1}. Both the position of the band and its height at mid-width were considered fit variables. Calculations were iterated until the best fit was obtained with $R^2 \geq 0.99$.

2.6. X-ray Diffraction (X-RD), Relative Crystallinity, and Crystallite Size

The XRD patterns of all samples were tested using a Bruker D8 Discover (AXS GmbH, Berlin, Germany) with Cu radiation at a wavelength of 1.5406 Å. Measurements were obtained at room temperature with a scanning rate of 0.02°/1 s and a diffraction angle range of 5 to 80° (2-theta range), where theta was the angle of incidence of the X-ray beam on the sample. The diffraction patterns were analyzed using EVA V. 5.1 software (Bruker, Berlin, Gernmany). XRD of frozen raw potato cubes (before being lyophilized) was carried out to compare the main effects of changes at the long-range level. The relative crystallinity was quantitatively estimated based on the relationship between the peak and total areas following the method of Nara and Komiya (1983) [25] using Origin software V. 9.5 (OriginLab Corporation, Northamton, United States). Starch crystallinity was calculated by:

$$[\text{crystalline area}/(\text{crystalline} + \text{amorphous}) \text{ area}] \times 100$$

The crystallite size was calculated using the Scherrer Equation (4) as described by Krauser et al., (2018) [26].

$$Cs = (0.94 \times \lambda)/(\beta \times \text{Cos } \theta)$$

where: Cs = average crystallite size, β = line broadening in radians, θ = Bragg angle, λ = X-ray wavelength.

2.7. Scanning Electron Microscopy (SEM)

Scanning electron microscopy (SERON SCI2100, Seron Technologies Inc., Uiwang-si, Republic of Korea) was used to visualize the surface structure of all the potato samples (raw, microwaved, and boiled; initially and after different intervals of drying). The samples were first subjected to vacuum in a vacuum chamber to be dehydrated and to prevent swelling under the microscope. Samples were then mounted on circular aluminum stubs with double-sided adhesive tape followed by 20 nm gold before observation. The SEM experiments were carried out at 15 KV × 4.0 K.

2.8. Statistical Analysis

Statistical analyses of the data were conducted using Minitab 20 (Minitab Inc., State College, PA, USA). The data concerning % of crystallinity and crystallite size were tested for significant differences ($p < 0.05$) using analysis of variance, one-way ANOVA, and Tukey's HSD comparison test.

3. Results and Discussion

3.1. Moisture Content

The moisture content for the potato samples was initially recorded to be 68.81%, 85.16%, and 85.27% for MP, BP, and RP, respectively, in accordance with other findings [27,28]. BP was reported to record values comparable to that of RP, as cooking was performed in water which facilitates the formation of hydrogen bonding within the starch granule. Microwaving potatoes resulted in the least initial moisture content, as the electromagnetic radiation targets the polar water molecules, causing them to oscillate and release water under intensive energy [6]. Moreover, a steeper water removal was detected

in the cooked samples compared to the raw sample (Figure 1), this could be explained by the structural changes induced upon heat treatment, causing gelatinization of starch and loosening the bond between the starch–starch and starch–protein network structures [28], thus facilitating the rapid removal of free water molecules at a faster rate (basically during the first 6 to 12 h of freeze drying in Bp and MP), beyond which both samples recorded a static value of moisture content, approximately 2.3% and 3.02% for MP and BP, respectively, majorly reflecting the percentage of adsorbed water.

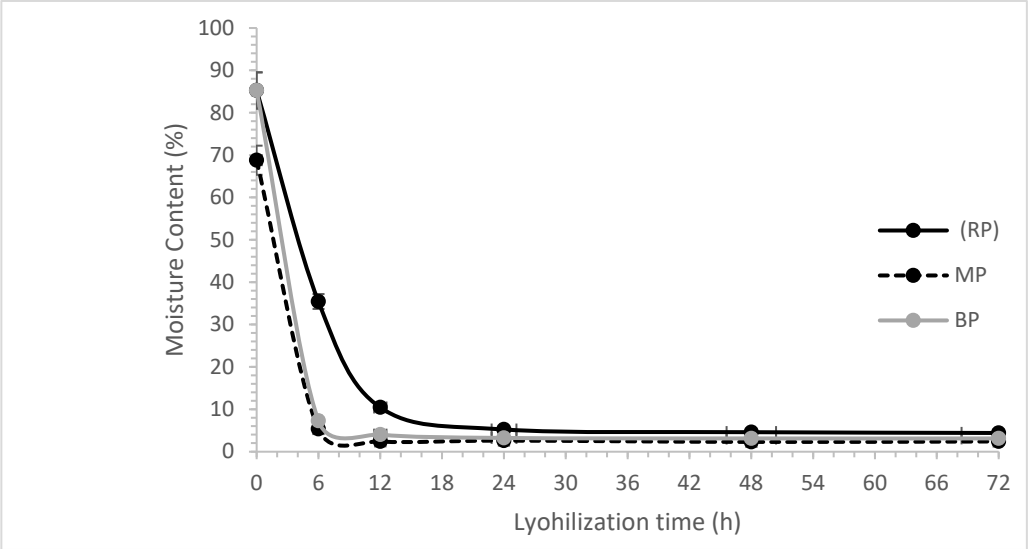

Figure 1. Moisture content % of MP, RP, and BP as a function of lyophilization time (h).

On the other hand, the presence of intact starch granules and the absence of heat treatment retarded the escape of water molecules from the raw potato tubers [1]. Almost all the free water was removed from RP after 24 h of freeze drying (Figure 1), which is in total confirmation with the SEM, FTIR, and XRD results as explained below. Beyond this value, RP recorded almost a constant value of moisture content around 4.5%, noting that this final value was statistically different than that obtained in BP and MP samples, which is again in confirmation with our results, indicating that RP samples would always adhere more adsorbed and bound water molecules within its structure.

3.2. Scanning Electron Microscopy (SEM)

SEM (Scanning Electron Microscope) images were utilized to detect microstructural alterations between RP, MP, and BP initially and following the various stages of freeze drying. Prior to freeze-drying (at t = 0), RP was seen to comprise clusters of intact starch granules that were oval in shape and had smooth surfaces of varying sizes (5–100 um) (Figure 2). This is a common characteristic of native potato starch granules [5,29–31]. After several hours (6 and 12) of freeze-drying, the quantity of starch granules in RP reduced, and they seemed to be encapsulated within the potato matrix.

This decrease in number could be the result of starch granule fracturing and the leaching out of starch molecular chains under the sublimation effect of freeze drying, starch de-structuring due to the removal of water.

LYOPHILISATION TIME T (HR)	RP	MP	BP
0	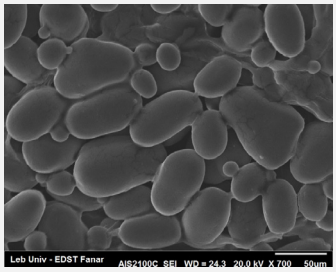	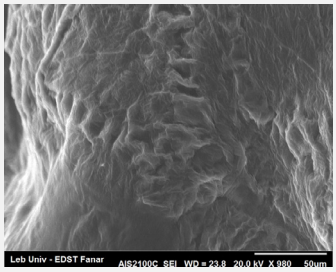	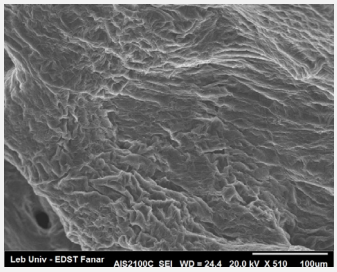
6	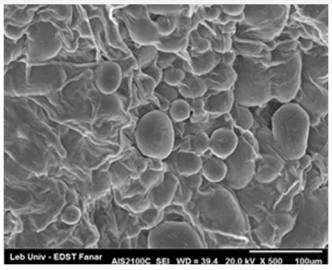	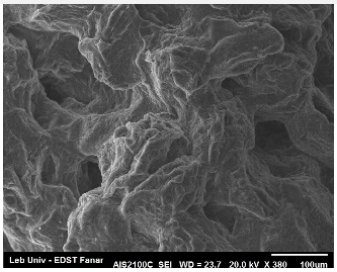	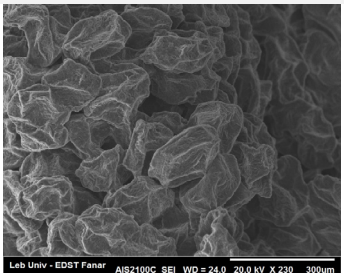
12	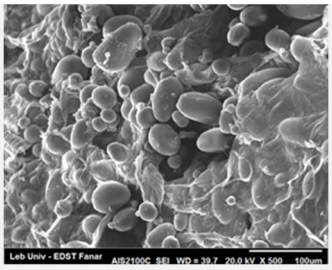	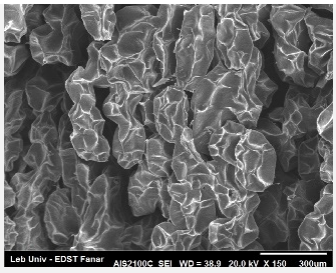	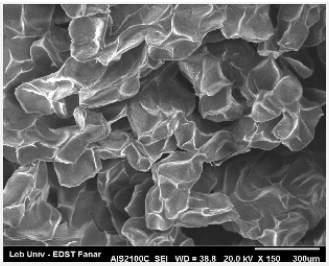
24	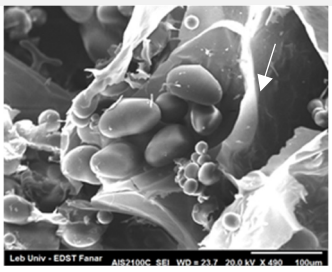	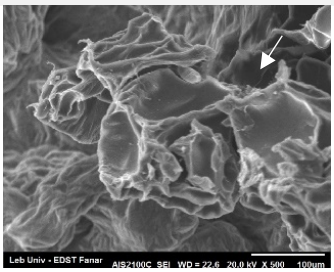	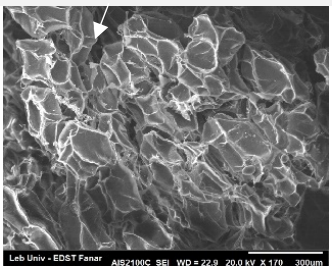
48	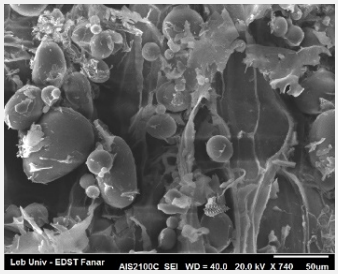	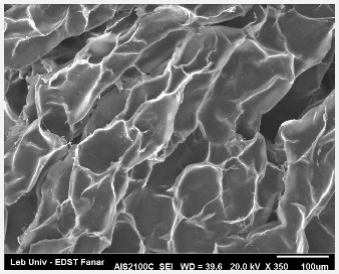	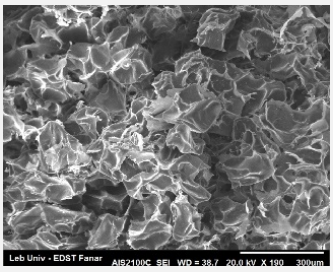

Figure 2. *Cont.*

72

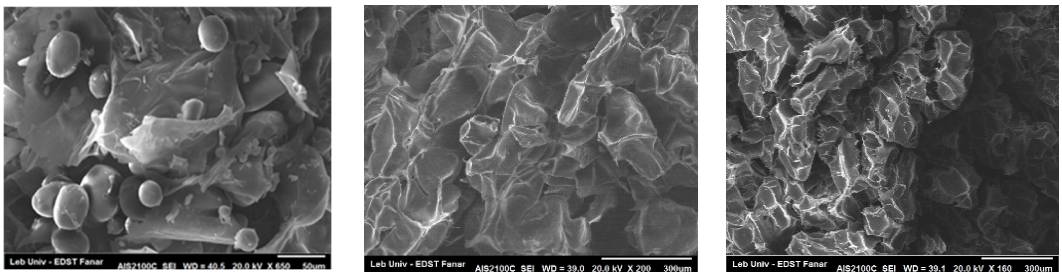

Figure 2. SEM micrographs of RP, MP, and BP at t_0 (initially before freeze-drying) and after 6, 12, 24, 48, and 72 h of freeze-drying respectively. Arrows correspond to the cavities induced inside the structure of potato due to freeze-drying.

RP samples marked main changes in the structural conformation after 24 h of freeze-drying, in confirmation with the moisture content result, where the major escape of water molecules was detected after 24 h of lyophilization. At this stage, RP24 showed a lower number of intact starch granules while others appeared dis-structured with ruptured cell walls, causing the starch to leach to a matrix that is now dried and fragile. Void cavities formed by the pushing force of water under freeze drying are also visible (Figure 2-RP 24 h). At the last stages of drying (72 h), the starch matrix appeared to be highly dried and brittle, with irregularly formed cracks due to extreme stress levels and extensive drying. Notably, very few starch granules were still detected in the RP72 sample but appeared to be rough, with visible scratches. The existence of some starch granules, albeit smaller in size, in RP samples after extensive freeze-drying for 72 h signifies the robustness of the molecular bonds in raw potato tubers between starch-starch molecules and starch-water molecules.

Conversely, SEM micrographs depicted significant structural variances between RP, MP, and BP from t = 0. It was evident that potatoes subjected to microwaving and boiling exhibited gelatinized starch granules (complete disappearance of starch granules due to heat treatment and cooking). As the duration of freeze-drying extended, BP revealed cells with fractured cell walls and fragments, as traditional treatment induces surface gelatinization in granules without disturbing the cellular structure [32].

Microwave treatment significantly alters the morphological structure of potato granules by stimulating through electromagnetic radiation the water molecules within the starch granules' crystalline regions, leading to enhanced rupture of the starch-lipid-protein complexes [33]. Freeze drying of both MP and BP resulted in the formation of smaller pores compared to those formed in RP24. Similarly, Wang et al. [34] observed that microwaving or boiling treatments prior to freeze-drying reduced the size of large cavities induced by the process. Moreover, BP that underwent 6 h of freeze drying exhibited an ordering process, visualized under the SEM by the emergence of edgy-like granules (Figure 2). This process involved starch re-association after initial gelatinization, followed by water removal and drying. Freeze drying facilitated the removal of water molecules, creating available binding sites and compacting the internal structure. This compacted structure promoted physical cross-linking between starch helixes, particularly the bonding between amylose and amylopectin. As a result, a reinforced network resembling the original starch-like granule structure was formed. Chen et al. [35] also stated that upon water removal, dispersed starch molecules go through a re-association process. With subsequent freeze drying, tearing of the surfaces was observed in both MP24 and BP24 samples. As drying progressed to 48 and 72 h, a highly compactable brittle polymer morphology with irregular fissure formation was evident in both MP and BP samples. Additionally, SEM images showed that the starch structure in BP samples was always denser, more compact, and more organized as the lyophilization time increased.

3.3. Fourier Transform Infrared Spectroscopy (FTIR)

3.3.1. Structural Analysis

Initially, at t = 0, the FTIR spectra of RP, BP, and MP indicated that the three samples shared most characteristic peaks, but with heat-treated samples (MP and BP) recording lower intensities than the original RP (Figure 3). This suggests that microwave heating and boiling had a major effect on reducing the number of helical structures present at the potato molecular structure. Similar results were reported by Fan et al. (2012) [36], who studied the effect of microwave heating and traditional heat drying on rice starch.

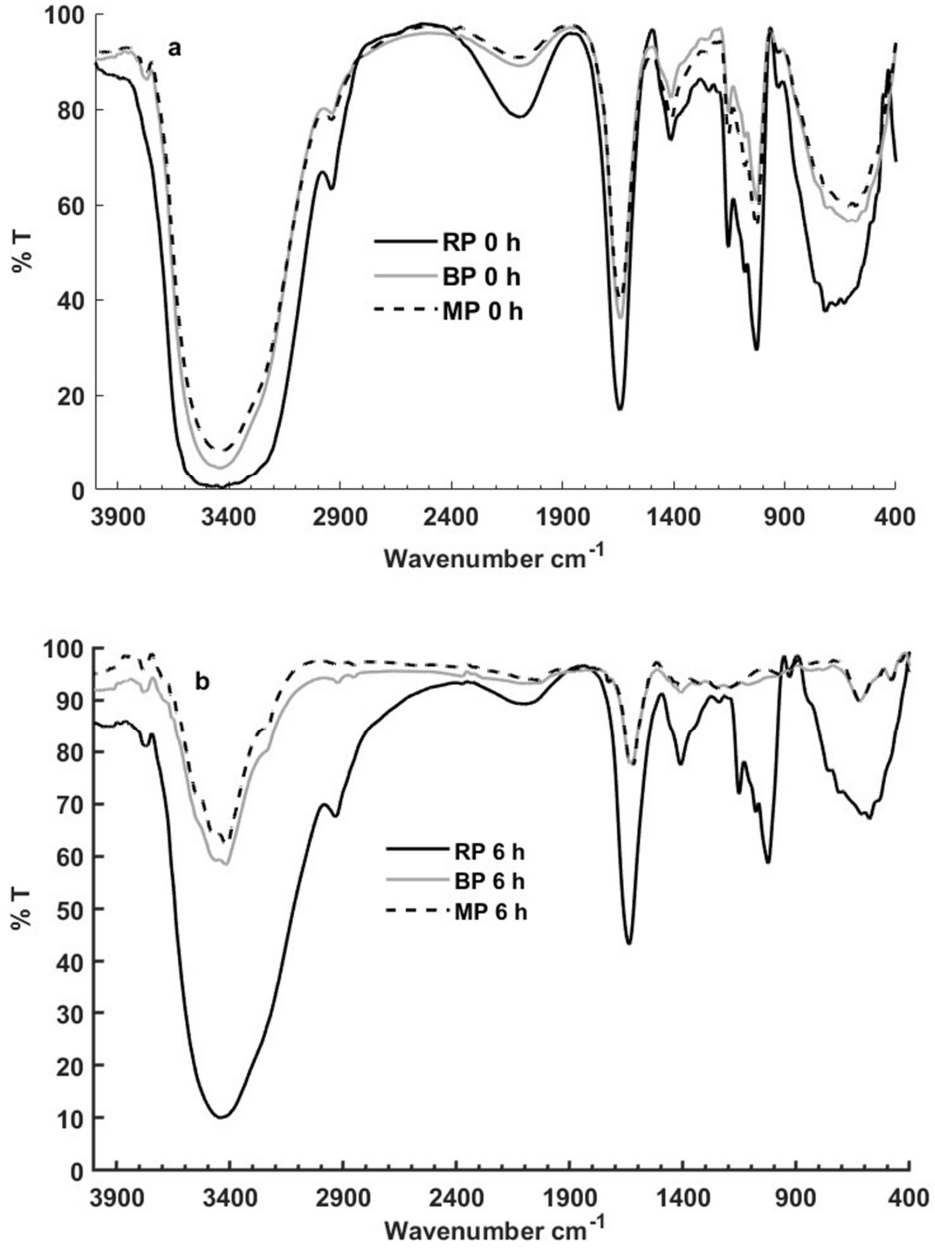

Figure 3. FTIR spectra for raw potato (RP), boiled potato (BP) and microwaved potato (MP) initially before freeze-drying (**a**) and after 6 h of freeze-drying (**b**).

As has been described by other authors, the three samples studied show the characteristic vibrations corresponding to: OH vibration (3500 cm^{-1}), CH_2 groups (2900 cm^{-1}), free water not bound to starch (2100 cm^{-1}), water molecules adsorbed in the amorphous region of starch (1650 cm^{-1}), CH_2 bending and -COO stretch (1412 cm^{-1}), vibration of the C-O-C glycosidic bond as well as the glucose ring (1160 cm^{-1}), ordered crystalline structure

(1048 cm^{-1}), amorphous structure (1022 cm^{-1}), vibrations of α 1–4 skeletal glycosidic bond (930 cm^{-1}), C-C stretch (750–600 cm^{-1} range), and skeletal modes of pyranose ring (577 cm^{-1}) (Figure 3) [2,18,28,36–40].

RP at t = 0 exhibited higher intensity for all peaks in comparison to BP and MP. This difference in intensity can be attributed to the processing treatments applied to the latter two samples (Figure 3a), which led to modifications in the inter and intra-molecular hydrogen bonds between starch molecules, or hydrogen bonds between water and proteins, consequently affecting the absorption intensity in the IR spectrum [36].

Significant shifts in peak positions between RP0, MP0, and BP0 were observed within the 1400–400 cm^{-1} range (fingerprint region), which is highly sensitive to changes in the structural conformation of starch. For instance, the peak at 715 cm^{-1} (representing C-C stretch) in RP0 shifted to 615 cm^{-1} in MP0, while the peak at 668 cm^{-1} (associated with skeletal modes of pyranose ring) shifted to 579 cm^{-1} in the BP0 and MP0 spectra (Figure 3a). These shifts indicated the impact of the applied heat treatment during processing on MP and BP, which corresponded to the physical differences observed in the SEM images. Previous studies have also reported changes in peak intensity within the 1400–400 cm^{-1} region due to processing [36,41].

After 6 h of freeze-drying, consistently dried spectra were observed for MP and BP, which remained similar throughout the rest of the drying period. This correlation was also observed in the moisture content results and the dried MP and BP SEM images after 6 h of freeze-drying (Figure 3b).

The strong interaction network among starch molecules (such as amylose-amylopectin and amylopectin-amylopectin intermolecular hydrogen bonds), as well as starch-water and starch-protein molecules in the RP sample, posed challenges in obtaining a dried spectrum through freeze drying. This process took 24 h, as evidenced by moisture content and SEM images. Interestingly, after 24 h of freeze-drying, the FTIR spectra of all three samples showed similarities to those of BP24 and MP24 (Figure 4).

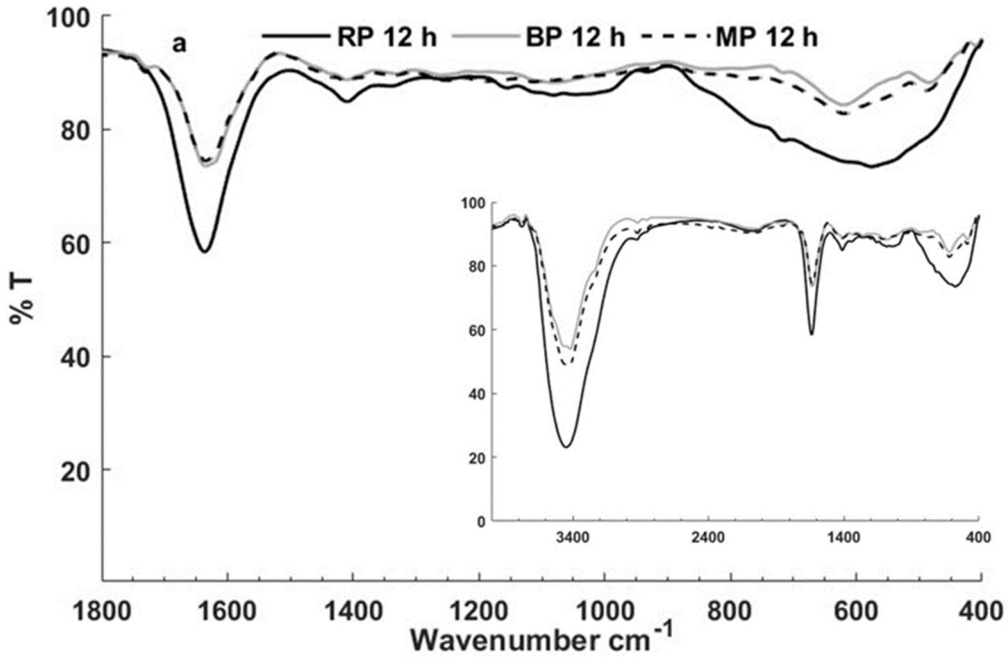

Figure 4. *Cont.*

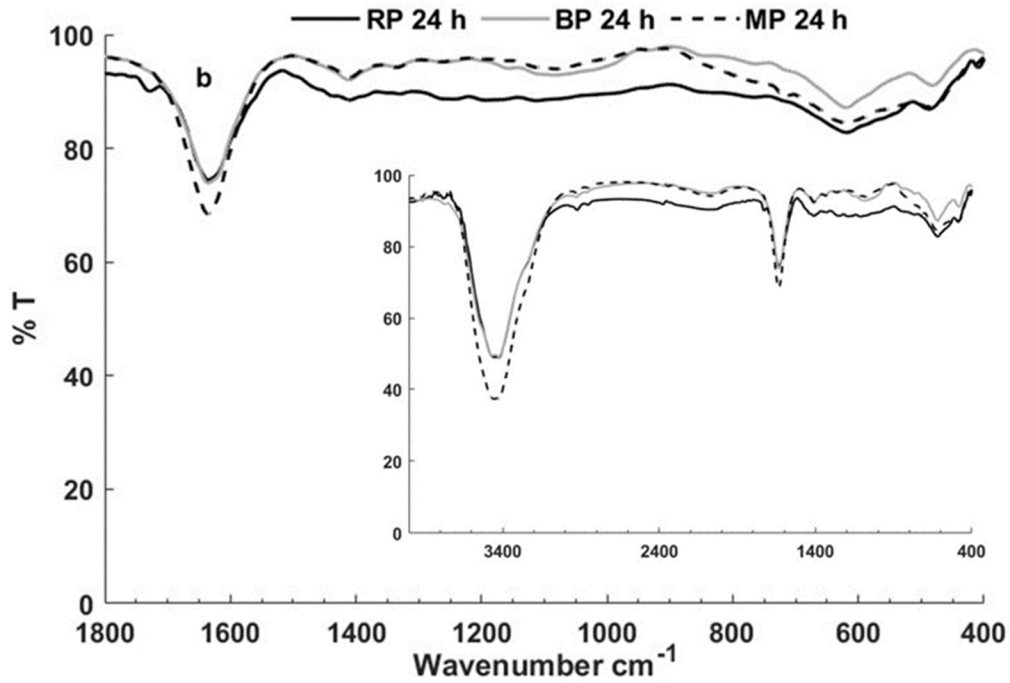

Figure 4. FTIR spectra for raw potato (RP), boiled potato (BP), and microwaved potato (MP) after 12 h (**a**) and 24 h (**b**) of freeze-drying.

Therefore, it was determined that a 24 h duration was necessary to remove the free water surrounding the helical structure of starch and protein in raw potato tubers (Figure 4b). The resulting structure in the potato samples consisted of the main integral skeletal structure of starch, and starch-protein with tightly bound water.

Conformational changes characterized by a significant decrease in the intensity of the peaks are induced by freeze drying, even disappearing some of them such as the 715 cm^{-1} peak in RP0 and the 1022 cm^{-1} peak in MP0 and BP0. In addition, a shift and narrowing are observed in other peaks as can be observed in the case of the MP and the BP samples. The shift of the peaks a observed from t = 0 to after 6 h of freeze drying: vibration of alpha 1–4 skeletal glycosidic bond (930 cm^{-1} to 970 cm^{-1}), skeletal modes of pyranose ring (597 cm^{-1} to 485 cm^{-1}), and C-C stretch (615 cm^{-1} to 620 cm^{-1}). In the case of the RP sample, the peaks shifts are observed from 632 cm^{-1} at t = 0 to 575 cm^{-1} at t = 12 h and 485 cm^{-1} at t = 24 h (skeletal modes of pyranose ring vibrations), and from 668 cm^{-1} at t = 0 to 620 cm^{-1} at t = 24 h (C-C stretch vibrations) (Figure 4). It is interesting to note that the peaks at 620 and 485 cm^{-1} have been observed in all the dried starch samples at different dehydration times, and therefore they could be assigned to the dehydrated starch skeleton (Figure 5). This assumption gains weight as the narrowing of the peaks (and thus the decrease in possible conformational configurations) coincides with the shift [42].

For a deeper understanding of the water molecules' presence vs. absence on the hydrogen bond networking and starch structuring, deconvolution of the FTIR results is developed as extended in the following section.

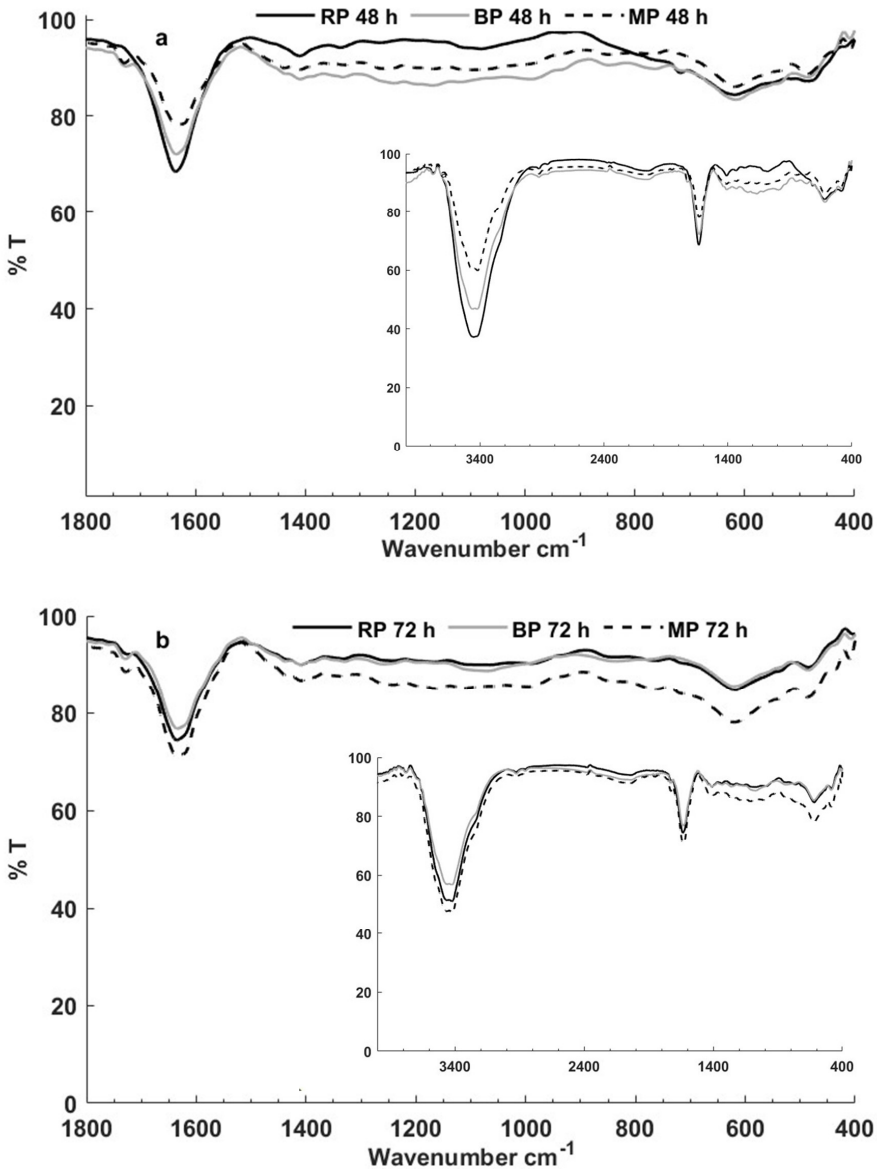

Figure 5. FTIR spectra for raw potato (RP), boiled potato (BP), and microwaved potato (MP) after 48 h (**a**) and 72 h (**b**) of freeze-drying.

3.3.2. Analysis of the Hydrogen Bond in Starch

The frequency of OH vibrations is known to decrease with the strength of the hydrogen binding (D. A. Schmidt and K. Miki, 2007 [24]) and can be interpreted as a change in the OH interaction distribution.

A detailed analysis of the vibrational modes ν(OH) of water bound to starch allows us to understand the role of starch–water interactions in the maintenance of the starch structure. The initial position of the bands was centered on the previously reported water OH bending and tension wave numbers, and this parameter was left as a variable during the adjustment. Figure 6 shows the deconvolution spectrum in the 3700–3000 cm^{-1} region of untreated starch (RP sample, freeze-drying times 0 h).

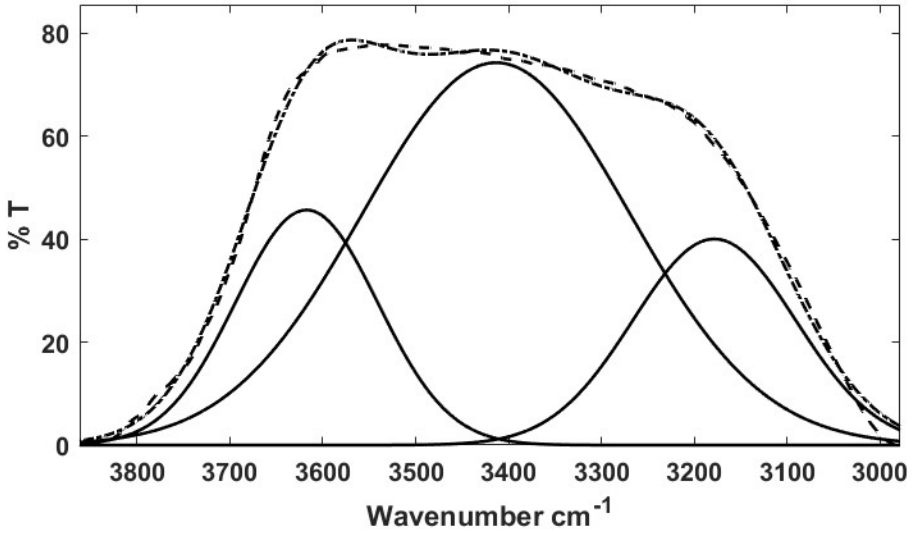

Figure 6. Curve fitting analysis of the un-lyophilized raw potato (RP 0 h sample). The figure displays the experimental FTIR signal (----), the simulated profile (-···-) and the three resolved components centered at 3618 cm^{-1}, 3414 cm^{-1} and 3180 cm^{-1}.

The best fit shows the three bands, centered at 3618, 3414, and 3180 cm^{-1}, in agreement with the results found by other authors. The band centered at 3618 cm^{-1} is assigned to very weak hydrogen bonds, the band centered at 3414 cm^{-1} has been assigned to medium hydrogen bonds, and the band centered at the lowest wavenumbers (3180 cm^{-1}) is assigned to strong or very strong hydrogen bonds [24]. The same deconvolution procedure has been performed for all the samples studied, at different freeze-drying times. Results are shown in Table 1. As was mentioned in the introduction section, and in agreement with our results, the presence of several kinds of water molecules also has been deduced from NMR results [43,44].

Table 1. The results from the curve fitting method applied to RP, BP, and MP at different freeze-drying times (Figure 5). For each sample, the wavelength position of the band component (column 1), the contribution in % of this band to the total absorption signal between 3800 cm^{-1} to 3000 cm^{-1} (column 2), and the best residual fits are shown.

	Samples								
	RP			**BP**			**MP**		
Freeze Drying Time (h)	**cm^{-1}**	**% ν(OH)**	**R^2**	**cm^{-1}**	**% ν(OH)**	**R^2**	**cm^{-1}**	**% ν(OH)**	**R^2**
0	3618 3414 3180	19.8 60.6 19.6	0.9972	3600 3457 3242	15.33 47.95 36.72	0.9982	3596 3448 3237	15.90 52.40 31.70	0.9976
6	3588 3447 3239	15.2 50.5 34.3	0.9986	3533 3412 3270	34.26 41.75 23.99	0.9989	3508 3399 3262	57.09 22.14 20.76	0.9974
12	3578 3445 3258	16.2 57.9 25.9	0.9996	3527 3398 3247	43.53 41.35 15.11	0.9990	3566 3438 3265	21.15 56.15 22.70	0.9994
24	3548 3424 3271	30.1 45.0 24.9	0.9995	3555 3427 3270	28.40 44.90 26.70	0.9993	3571 3432 3236	15.93 72.04 12.03	0.9996

Table 1. *Cont.*

	Samples								
	RP			BP			MP		
Freeze Drying Time (h)	**cm^{-1}**	**% ν(OH)**	**R^2**	**cm^{-1}**	**% ν(OH)**	**R^2**	**cm^{-1}**	**% ν(OH)**	**R^2**
48	3559	27.8	0.9996	3564	23.30	0.9994	3549	30.09	0.9991
	3426	47.6		3431	55.40		3421	50.56	
	3262	24.6		3256	21.30		3256	19.35	
72	3555	25.0	0.9994	3533	39.20	0.9993	3548	33.22	0.9992
	3430	49.33		3412	38.70		3421	41.19	
	3267	25.63		3263	22.10		3268	25.59	

Comparing the three samples before freeze-drying (at t = 0 h), a variation in the position of the band centered at 3600 cm^{-1} is observed, which, being indicative of changes in the distribution of the OH bond strengths, could reflect structural changes at the molecular level induced by the thermal treatments, contrary to what was proposed by D. Fan et al., [36] The shift to lower wavenumbers of this band in the case of the heat-treated samples compared to the untreated one is a characteristic of the removal of the more superficial, free, and weakly bound water molecules from the helical structure due to heat treatment. This is in perfect agreement with the decrease in the intensity of the band centered between 3700 and 3000 cm^{-1} of the heat-treated and non-lyophilized samples, compared to the non-heat-treated and non-freeze-drying samples (Figure 6).

The reason that D. Fan et al., [36] did not find differences between the microwaved and boiled starch samples may be due to the fact that their FTIR spectra are very similar (Figure 6), and a deeper analysis is necessary, as in this case, the study of changes in the strengths of OH bonds. In this sense, the study of the complex structure of the OH vibration bands can provide information about the H-bond network and how it is or can be modified by different treatments such as thermal exposure, cooking methods, or lyophilization.

Figure 7a shows the shift in the position of the wavenumber of each of the three OH bands at 3700–3000 cm^{-1} FTIR region as a function of the freeze-drying times, taken from the values in Table 1. It is observed that there is a shift in the wavenumber in the first hours (6–12 h) in the case of thermally treated samples (BP and MP), while in the case of RP, these changes are slower and occur after 24 to 48 h. In all samples, the shifts of the three bands converge to approximately the same wavenumber: 3550 cm^{-1}, 3425 cm^{-1}, and 3225 cm^{-1}. The convergence to the same wave number could be indicative that the changes induced by the different thermal treatments followed by freeze-drying lead to a very similar molecular structure in the three samples studied.

Figure 7b illustrates that the peak centered at 1640 cm^{-1}, corresponding to the bending vibration of OH bonds, exhibits a similar trend to the peaks in the OH bond stretching region. With increasing freeze-drying time, there is a decrease in intensity and a shift to lower wavenumbers. These changes are attributed to water removal and alterations in hydrogen bond strengths. In the heat-treated samples (BP and MP), these intensity and wavenumber changes occur within the first hours (6–12). However, in the case of the untreated sample (RP), these changes become apparent after 24 and 48 h, aligning well with the observed alterations in the region of water stretching vibration (3700–3000 cm^{-1}).

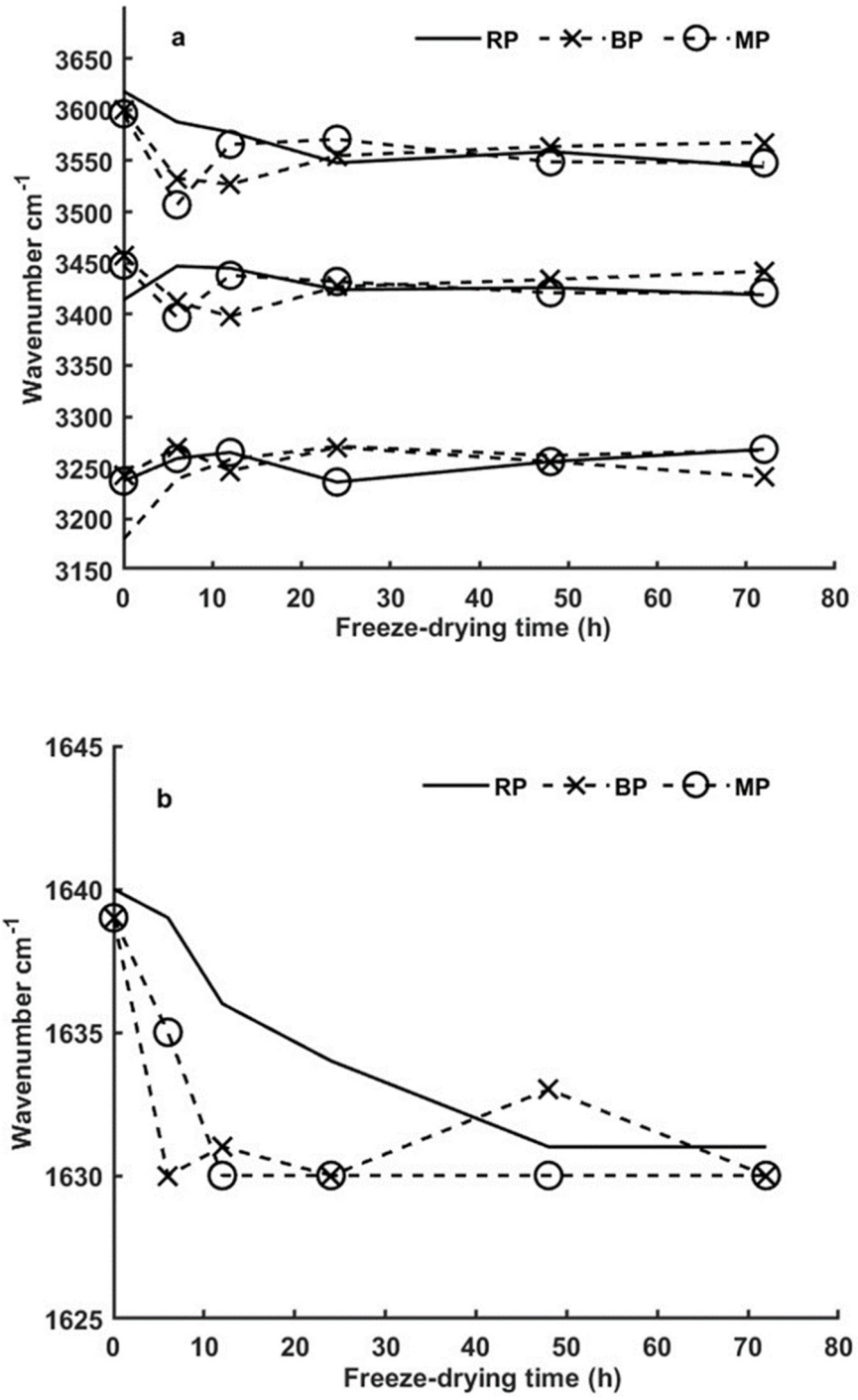

Figure 7. Wavenumber shift of the 3 peaks corresponding to the OH vibration in the 3700–3000 cm^{-1} region (**a**) and that of the peak centered at 1640 cm^{-1} that corresponds to the OH bending vibration (**b**), as a function of the freeze-drying time (h).

Although the peak centred at 1650 cm^{-1} has been widely assigned to the OH group vibration, and water is a molecule present in much greater quantity than proteins, it is possible that this peak also contains vibration corresponding to the amide region of proteins. The fact that this peak does not disappear completely is compatible both with the presence of OH bonds and with the presence of C=C, C=O, and C=N groups of denatured or partially denatured proteins.

3.4. X-ray Diffraction (XRD)

The broad peak observed in the RP0 at 2θ = 30° to 40° is indicative of a predominantly amorphous structure. This is consistent with previous studies, which have reported that native potato starch granules typically exhibit a less ordered crystalline structure due to the presence of a high amylopectin content and less compact arrangement of starch molecules [45]. The amorphous regions contribute to the broad nature of the peak, as opposed to sharp diffraction peaks characteristic of highly crystalline materials.

The sharp peak at 2θ = 27° observed in both MP0 and BP0 samples suggests a significant increase in crystalline order due to the heating processes. This observation correlates with the literature, where thermal processing is known to induce structural changes in starch granules, promoting reorganization and crystallization [46].

Specifically, microwaving and boiling can cause gelatinization of starch, where the granules swell, crystalline regions melt, and molecular realignment occurs upon cooling. This process enhances the crystalline nature of the starch, as evidenced by the emergence of more defined peaks in the XRD patterns [47]. The peak at 2θ = 27° is characteristic of B-type crystallinity, which is common in tuber starches and indicates the formation of more ordered crystalline domains [48].

The transformation from a predominantly amorphous structure in raw potato starch to a more crystalline structure upon heating aligns well with the findings of Bogracheva et al. [49], who noted similar changes in pea starch. This transformation is often attributed to the disruption of native starch granules and the subsequent formation of new crystalline regions as the starch molecules reassociate in a more ordered manner during cooling [49].

After 6 h of freeze-drying, the XRD patterns of MP displayed similar shapes, although with slight variations in intensity, appearing almost superimposed. Similarly, for RP, comparable XRD patterns were observed after 24 h of freeze-drying. These findings support the previous hypothesis that MP reaches a dried state after 6 h, while RP requires more time (24 h) to fully dry (Figure 8).

Furthermore, a shift in the 2-theta angle was observed in RP after 24 h of freeze-drying and in MP after 6 h, indicating significant alterations in the starch structure at these specific drying times. Based on these observations, MP6 and RP24 were identified as completely dried samples, confirming the previous results.

Additionally, the XRD pattern of RP24 exhibited a noticeable alteration, marked by the emergence of two peaks corresponding to native potato starch (with low B-type crystallinity) at 2-theta = 17° and 22° [50]. These peaks gradually intensified until the end of the freeze-drying stages, indicating a transformation in the structure of RP starting from 24 h.

On the other hand, an increase in the XRD peak was observed in BP after 6 h of freeze-drying, indicating an increase in structural ordering. It was also noted that BP0 and BP6 exhibited the same 2-theta angle level, which undergoes a shift after only 12 h of freeze-drying, suggesting major structural changes and the emergence of a dried skeletal structure in BP samples. According to R. Wang et al. [34] a shift in the 2-theta angle signifies a deeper change at the level of the unit cell dimension.

The XRD patterns of the MP, BP, and RP samples show changes in their intensities that may be due to conformational changes (long-range order), as shown in the SEM images (Figure 8).

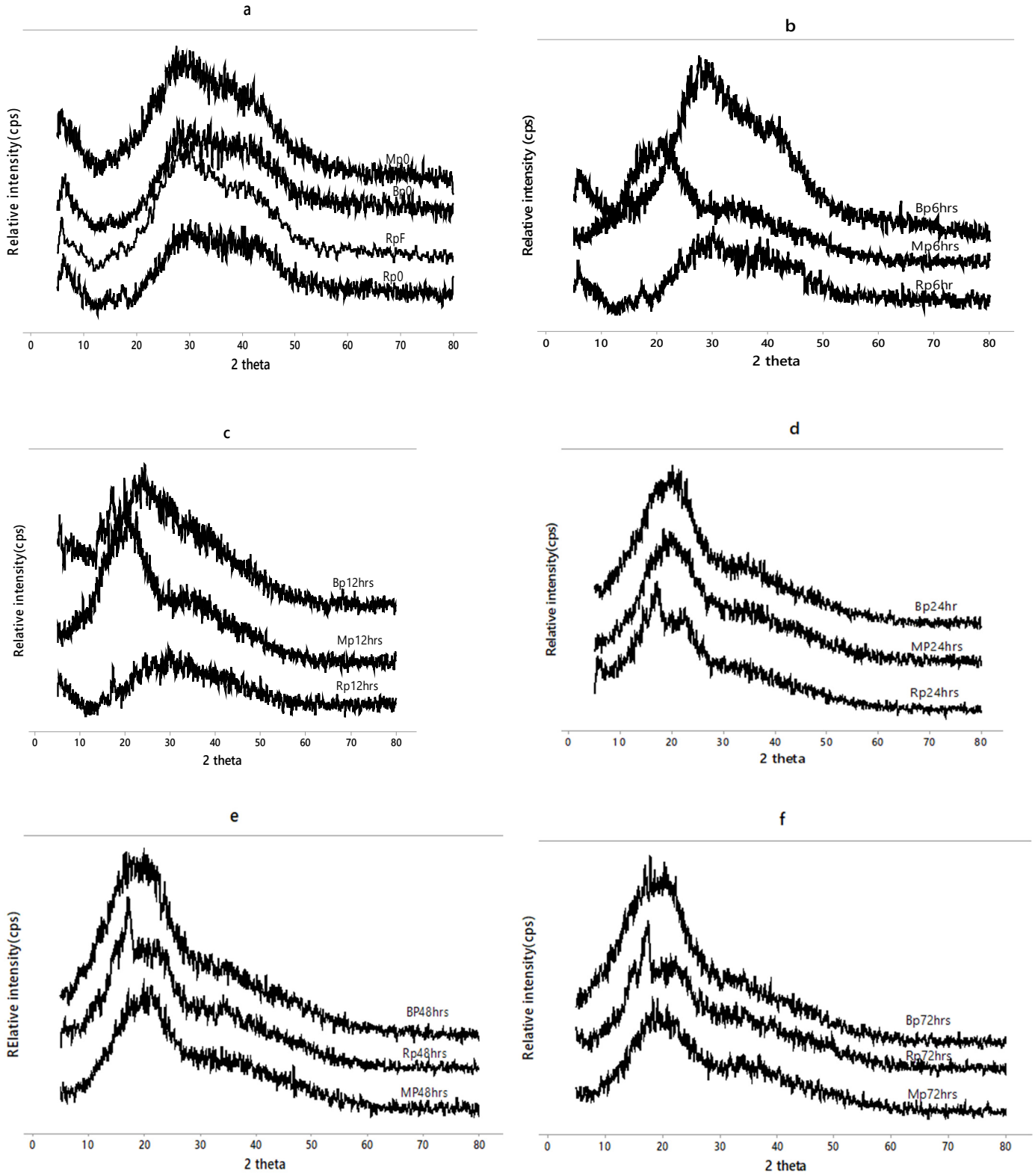

Figure 8. XRD patterns of RP0, BP0, MP0 (initially before freeze-drying), and RPF (after lyophilization) (**a**), and XRD patterns of RP, BP, and MP after 6 h (**b**), 12 h (**c**), 24 h (**d**), 48 h (**e**) and 72 h (**f**) of freeze-drying respectively.

In this sense, the BP sample has a peak of higher intensity than that of the MP sample after 6 h of freeze-drying, which persists for the rest of the drying stages. This difference may be due to a conformational reorganization of starch and proteins into a granular

structure in the BP samples. Compared to the MP samples, a more compact and dense structure is detected. These results are corroborated by the relative crystallinity calculations.

All the crystallinity % of the differently treated samples falls in the range of 19 to 32% (Figure 9), which is in accordance with the other authors reporting the % of crystallinity in potato starch [51,52].

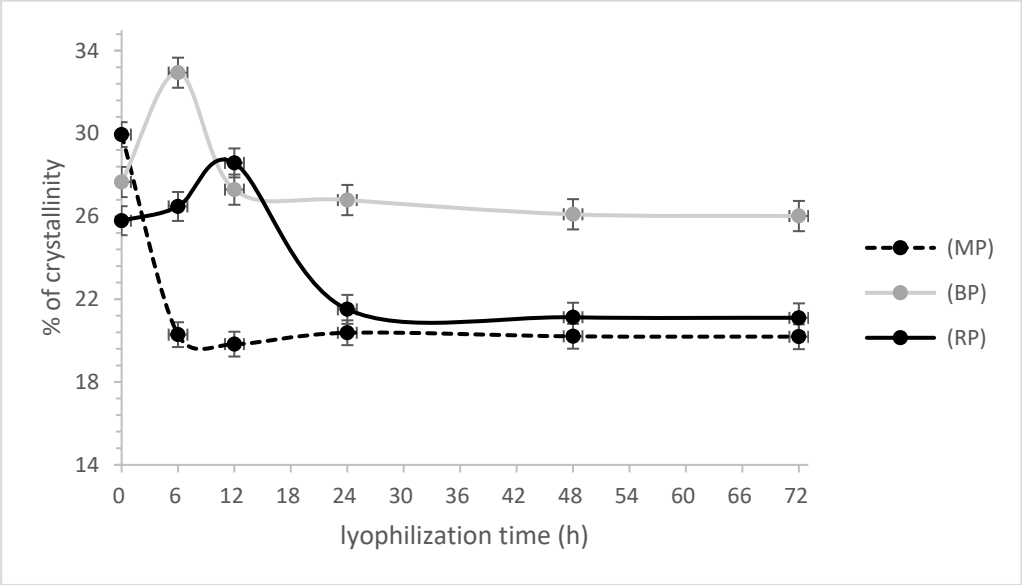

Figure 9. Relative % of crystallinity of MP, RP and BP as a function of lyophilization time (h).

The % of crystallinity comes in agreement to verify the results obtained in the analysis of H-bonds changes revealed via FTIR. Thermal treatment showed a significant difference in % of crystallinity, displaying a higher value compared to untreated samples (RP), this could be explained as temperature triggers the hydrogen bonds, inducing malleability and allowing starch helixes to reassociate into a more ordered structure. Additionally, the type of cooking treatment showed a significant difference with microwaving recording higher crystallinity percentages compared to boiling. This could be partially attributed to the vibration of the molecules induced by the microwave electromagnetic radiation allowed for the re-alignment of amylose chains and/or its reassessment with other constituents such as amylose-protein or amylose-lipid complexes as defined by [52]. L. Wang et al. [51] also found an increase in the relative crystallinity (RC) of potato starch after microwave treatment. Comparing both cooking treatments, microwaving is less disruptive [39], electromagnetic radiation directly targets -OH bonds (water molecules) whereas boiling treatment affects all the molecular bonds including C-C starch and -OH bonds, inducing a less ordered structure expressed by lower RC (Figure 9).

Moreover, the physiological process of freeze drying (lyophilization) affects the RC of the samples differently. MP showed an abrupt decrease in RC by 33% during the first 6 h of lyophilization (Figure 9), as most of the water molecules become loosely attached after being exposed to the electromagnetic radiation, which facilitates its instantaneous and whole release once freeze-drying is applied, leading to less alignment between the amylose and amylopectin starch helices and consequently a lower degree of crystallinity [53,54]. This hypothesis was confirmed as further stages of lyophilization post 6 h kept the same RC~20%, indicating stability in the structural changes, and that almost all the water molecules were removed before 6 h and little to no water molecules are further detached. To the contrary BP showed an increase of 19.09% in RC during the first 6 h of freeze drying, this value decreased back after 12 h and remained constant throughout the stages (Figure 9). During boiling, potatoes are hydrolyzed as additional water molecules penetrate from the cooking media and are dispersed between cleaved starches, in this case aiding in a less organized medium.

Consequently, the partial removal of this water by freeze drying enables more space for the re-association of starch chains and recrystallization ordering. At 12 h of lyophilization, the additional removal of water from BP samples caused a disruption in the order revealed by a lower level of crystallinity [53,54]. However, BP showed significantly higher levels of RC starting 24 h till the end of the lyophilization, explaining the denser, more compact structure that was also revealed via SEM images. The changes of RC among RP at different freezing times were observed to be gradual due to the presence of a definitive structure. At 24 h, the RC of RP recorded a drop by ~25%, where it is stabilized thereafter. Notably, the RC of MP and RP align ideally and show no significant difference post-24 h of lyophilization (Figure 9). In contrast to Chen et al. [55], who stated that freeze drying increased the range ordering and RC of starch in yam flours, it was found that RC decreases for all the samples with high intensity of water removal during lyophilization As microwaving was found to induce less chemical modifications than that of boiling, the intensity of lyophilization aids in adhering the MP starch structure to that of unprocessed raw potato. A common thing among all the samples is that changes are stabilized post 24 h of lyophilization, indicating that only strongly bound water molecules (unremovable) are still present, in agreement with the FTIR results.

Crystallite size as a function of thermal treatment and intensity of water removal is assessed in Table 2. Crystallite size is related to its perfection, in a way that an increase in crystallite size indicates the formation of a more perfect crystalline structure [26]. Thermal effect and cooking treatment on crystallite size were significantly different. Temperature reduces the crystallite size with the boiling treatment being more intense in this aspect, indicating more quantity of defect as described by [55] and in agreement with the previous assumptions derived in the % of crystallinity. Again, the crystallite size of MP showed a steep decrease of ~60% after 6 h of lyophilization, indicating a rapid disordering in structure in just a little time, whereas BP displayed a ~54% decrease in crystallite size after 12 h of lyophilization. Only RP at 12 h showed an increase in crystallite size by ~60%, beyond which the crystallite size decreases largely to stabilize at around ~1 nm. This could be explained by the fact that the first stages of freeze-drying increased chain mobility in raw samples which allows for a larger number of encounters between the chains, favoring nucleation and so leading to the formation of larger, more perfect crystallites.

Table 2. Average crystallite size of Rp, MP, and BP as a function of lyophilization time (h) using Scherrer equation, fitting with a Gaussian curve, R^2 = 0.989–0.993.

	The Average Crystallite Size (nm)		
Lyophilization Time (h)	**(RP)**	**(MP)**	**(BP)**
0	1.602 ± 0.158^{b}	$1.32 \pm 0.035^{b,c,d}$	$0.856 \pm 0.024^{e,f,g}$
6	$1.077 \pm 0.064^{c,d,e}$	$0.550 \pm 0.022^{g,h,i}$	$0.740 \pm 0.016^{f,g,h}$
12	2.570 ± 0.238^{a}	$0.595 \pm 0.038^{f,g,h,i}$	0.388 ± 0.031^{i}
24	$1.190 \pm 0.267^{b,c}$	$0.523 \pm 0.01^{h,i}$	0.383 ± 0.015^{i}
48	$0.946 \pm 0.099^{d,e}$	$0.522 \pm 0.013^{h,i}$	0.389 ± 0.024^{i}
72	$0.928 \pm 0.162^{e,f}$	$0.545 \pm 0.011^{g,h,i}$	0.388 ± 0.017^{i}

a–i, different letters indicate a significant difference between crystallite size, and a common letter indicates no significant difference.

Industrially, a higher RC in starch is related to higher levels of hardness and density whereas larger crystallite sizes induce higher thermal stability in samples [43,52,55], relatively, each tested sample could serve as an ideal candidate in industrial processing according to the manufacturing purpose.

4. Conclusions

This study highlights the pivotal role of water molecules in preserving the structural integrity of potato starch. Even after a 72 h freeze-drying process, water molecules remain

firmly associated with starch in raw potato tubers, as confirmed by FTIR analysis and the presence of smaller starch granules in the samples. Additionally, the removal of water molecules induces a conformational change analogous to heat treatments, as evidenced by the distribution of hydrogen bond energies after 72 h of freeze-drying.

Various types of hydrogen bonds between water and starch were identified, categorized as weak (around 3600 cm^{-1}), medium (around 3400 cm^{-1}), and strong (around 3200 cm^{-1}). The study provides detailed insights into how these bonds change with cooking treatment and the degree of lyophilization.

Examining hydrogen bonds offers a molecular-level understanding of structural alterations in potato starch–protein interactions. Heat-treated samples exhibited a decrease in free or weakly bound water compared to non-heat-treated samples. Peak shifts in the fingerprint region were observed across all samples, and two distinct peaks at approximately 485 cm^{-1} and 620 cm^{-1} were consistently identified as characteristic of dried potato starch.

Freeze drying resulted in reduced starch molecule order, evident through decreased relative crystallinity and crystallite size.

By combining cooking methods with freeze-drying, we obtained samples with various industrial applications. BP retained higher crystallinity and smaller crystal size after freeze drying, making it a suitable material for manufacturing dense, brittle products. Lyophilized MP exhibited relatively larger crystallite sizes and a relative crystallinity comparable to RP, making it a more pliable material for industrial processes.

Author Contributions: Material preparation, data collection and analysis were performed by I.D. and F.S. Project management was performed by A.H., M.P. and F.S. The first draft of the manuscript was written by I.D. and all authors commented on previous versions of the manuscript. Final manuscript revision was performed by I.D. and F.S. All authors have read and agreed to the published version of the manuscript.

Funding: Erasmus+ KA171 for international mobility. Project 2022-2025.

Institutional Review Board Statement: Not applicable.

Data Availability Statement: Dataset generated during the current study are available from the corresponding author upon reasonable request.

Conflicts of Interest: The authors declare no conflicts of interest.

References

1. Reyniers, S.; Ooms, N.; Gomand, S.V.; Delcour, J.A. What makes starch from potato (*Solanum tuberosum* L.) tubers unique: A review. *Compr. Rev. Food Sci. Food Saf.* **2020**, *19*, 2588–2612. [CrossRef] [PubMed]
2. Dankar, I.; Haddarah, A.; Omar, F.E.; Pujolà, M.; Sepulcre, F. Characterization of food additive-potato starch complexes by FTIR and X-ray diffraction. *Food Chem.* **2018**, *260*, 7–12. [CrossRef] [PubMed]
3. Eghbaljoo, H.; Sani, I.K.; Sani, M.A.; Rahati, S.; Mansouri, E.; Molaee-Aghaee, E.; Fatourehchi, N.; Kadi, A.; Arab, A.; Sarabandi, K.; et al. Advances in plant gum polysaccharides; Sources, techno-functional properties, and applications in the food industry—A review. *Int. J. Biol. Macromol.* **2022**, *222*, 2327–2340. [CrossRef] [PubMed]
4. Jayanty, S.S.; Diganta, K.; Raven, B. Effects of Cooking Methods on Nutritional Content in Potato Tubers. *Am. J. Potato Res.* **2019**, *96*, 183–194. [CrossRef]
5. Romano, A.; D'Amelia, V.; Gallo, V.; Palomba, S.; Carputo, D.; Masi, P. Relationships between composition, microstructure and cooking performances of six potato varieties. *Food Res. Int.* **2018**, *114*, 10–19. [CrossRef]
6. Oyeyinka, S.A.; Akintayo, O.A.; Adebo, O.A.; Kayitesi, E.; Njobeh, P.B. A review on the physicochemical properties of starches modified by microwave alone and in combination with other methods. *Int. J. Biol. Macromol.* **2021**, *176*, 87–95. [CrossRef]
7. Yang, Y.; Achaerandio, I.; Pujolà, M. Effect of the intensity of cooking methods on the nutritional and physical properties of potato tubers. *Food Chem.* **2016**, *197*, 1301–1310. [CrossRef]
8. Ormerod, A.; Ralfs, J.; Jobling, S.; Gidley, M. The influence of starch swelling on the material properties of cooked potatoes. *J. Mater. Sci.* **2002**, *7*, 1667–1673. [CrossRef]
9. Singh, N.; Kaur, L.; Ezekiel, R.; Guraya, H.S. Microstructural, cooking and textural characteristics of potato (*Solanum tuberosum* L) tubers in relation to physicochemical and functional properties of their flours. *J. Sci. Food Agric.* **2005**, *85*, 1275–1284. [CrossRef]
10. Fedec, P.; Ooraikul, B.; Hadziyev, D. Microstructure of Raw and Granulated Potatoes. *Can. Inst. Food Sci. Technol. J.* **1977**, *10*, 295–306. [CrossRef]

11. Wang, B.; Chen, S.; Huang, C.; Lin, Y.; Liang, Y.; Xiong, W.; Zhang, B.; Liu, R.; Ding, L. Comparative study on the structural and in vitro digestion properties of starch within potato parenchyma cells under different cooking methods. *Int. J. Biol. Macromol.* **2022**, *223*, 1443–1449. [CrossRef] [PubMed]
12. Cameron, D.K.; Wang, Y.-J. A Better Understanding of Factors That Affect the Hardness and Stickiness of Long-Grain Rice. *Cereal Chem.* **2005**, *82*, 113–119. [CrossRef]
13. Van Soest, J.J.; Hulleman, S.H.D.; De Wit, D.; Vliegenthart, J.F.G. Crystallinity in strach bioplastics. *Ind. Crop. Prod.* **1996**, *5*, 11–22. [CrossRef]
14. Yang, S.; Dhital, S.; Shan, C.S.; Zhang, M.N.; Chen, Z.G. Ordered structural changes of retrograded starch gel over long-term storage in wet starch noodles. *Carbohydr. Polym.* **2021**, *270*, 118367. [CrossRef]
15. Olad, A.; Doustdar, F.; Gharekhani, H. Fabrication and characterization of a starch-based superabsorbent hydrogel composite reinforced with cellulose nanocrystals from potato peel waste. *Colloids Surf. A Physicochem. Eng. Asp.* **2020**, *601*, 124962. [CrossRef]
16. Kaláb, M.; Allan-Wojtas, P.; Miller, S.S. Microscopy and other imaging techniques in food structure analysis. *Trends Food Sci. Technol.* **1995**, *6*, 177–186. [CrossRef]
17. Flores-Morales, A.; Jiménez-Estrada, M.; Mora-Escobedo, R. Determination of the structural changes by FT-IR, Raman, and CP/MAS 13C NMR spectroscopy on retrograded starch of maize tortillas. *Carbohydr. Polym.* **2012**, *87*, 61–68. [CrossRef]
18. Zhang, N.; Liu, X.; Yu, L.; Shanks, R.; Petinaks, E.; Liu, H. Phase composition and interface of starch–gelatin blends studied by synchrotron FTIR micro-spectroscopy. *Carbohydr. Polym.* **2013**, *95*, 649–653. [CrossRef]
19. Ma, Y.; Chen, Z.; Wang, Z.; Chen, R.; Zhang, S. Molecular interactions between apigenin and starch with different amyl ose/amylopectin ratios revealed by X-ray diffraction, FT-IR and solid-state NMR. *Carbohydr. Polym.* **2023**, *310*, 120737. [CrossRef]
20. Battistel, M.D.; Pendrill, R.; Widmalm, G.; Freedberg, D.I. Direct evidence for hydrogen bonding in glycans: A combined NMR and molecular dynamics study. *J. Phys. Chem. B* **2013**, *117*, 4860–4869. [CrossRef]
21. Kumar, Y.; Singh, L.; Sharanagat, V.S.; Patel, A.; Kumar, K. Effect of microwave treatment (low power and varying time) on potato starch: Microstructure, thermo-functional, pasting and rheological properties. *Int. J. Biol. Macromol.* **2020**, *155*, 27–35. [CrossRef] [PubMed]
22. Van Soest, J.J.; Hulleman, S.H.D.; De Wit, D.; Vliegenthart, J.F.G. Changes in the mechanical properties of thermoplastic potato starch in relation with changes in B-type crystallinity. *Carbohydr. Polym.* **1996**, *29*, 225–232. [CrossRef]
23. AACC. Approved Methods of Analysis; Method 44-15.02: Moisture–Air-Oven Methods. Available online: https://www.bing.com/ck/a?!&&p=9568e7a101cc1a9aJmltdHM9MTcyODA4NjQwMCZpZ3VpZD0wMDkzMzc4Yy03MThhLTZlOTctMjFiMy0yNjgzNzA0YTZmZWUmaW5zaWQ9NTE4NA&ptn=3&ver=2&hsh=3&fclid=0093378c-718a-6e97-21b3-2683704a6fee&psq=AACC.+Approved+Methods+of+Analysis;+Moisture%E2%80%93Air-Oven+Methods+for+moisture+content.+references&u=a1aHR0cHM6Ly93d3cuY2VyZWFsc2dyYWlucy5vcmcvcmVzb3VyY2VzL01ldGhvZHMvUGFnZXMvZGVmYXVsdC5hc3B4&ntb=1 (accessed on 5 October 2024).
24. Schmidt, D.A.; Miki, K. Structural Correlations in Liquid Water: A New Interpretation of IR Spectroscopy. *J. Phys. Chem. A* **2007**, *111*, 10119–10122. [CrossRef] [PubMed]
25. Nara, S.; Komiya, T. Studies on the Relationship between Water-saturated State and Crystallinity by the Diffraction Method for Moistened Potato Starch. *Starch Stärke* **1983**, *35*, 407–410. [CrossRef]
26. de Oliveira Krauser, M.; de Souza Oliveira, H.H.; Cebim, M.A.; Davolos, M.R. Relationship between scintillation properties and crystallite sizes in Y2O3:Eu3+. *J. Lumin.* **2018**, *203*, 100–104. [CrossRef]
27. Decker, E.A.; Ferruzzi, M.G. Innovations in food chemistry and processing to enhance the nutrient profile of the white potato in all forms. *Adv. Nutr.* **2013**, *4*, 345S–350S. [CrossRef]
28. Andersson, A.; Gekas, V.; Lind, I.; Oliveira, F.; Öste, R.; Aguilfra, J.M. Effect of Preheating on Potato Texture. *Crit. Rev. Food Sci. Nutr.* **1994**, *34*, 229–251. [CrossRef]
29. Szymońska, J.; Krok, F.; Komorowska-Czepirska, E.; Rebilas, K. Modification of granular potato starch by multiple deep-freezing and thawing. *Carbohydr. Polym.* **2003**, *52*, 1–10. [CrossRef]
30. Yadav, A.R.; Guha, M.; Tharanathan, R.N.; Ramteke, R.S. Changes in characteristics of sweet potato flour prepared by different drying techniques. *LWT Food Sci. Technol.* **2006**, *39*, 20–26. [CrossRef]
31. Zhang, B.; Wang, K.; Hasjim, J.; Li, E.; Flanagan, B.M.; Gidley, M.J.; Dhital, S. Freeze-drying changes the structure and digestibility of B-polymorphic starches. *J. Agric. Food Chem.* **2014**, *62*, 1482–1491. [CrossRef]
32. Bouchon, P.; Aguilera, J.M. Microstructural analysis of frying potatoes. *Int. J. Food Sci. Technol.* **2001**, *36*, 669–676. [CrossRef]
33. Xie, Y.; Yan, M.; Yuan, S.; Sun, S.; Huo, Q. Effect of microwave treatment on the physicochemical properties of potato starch granules. *Chem. Cent. J.* **2013**, *7*, 1–7. [CrossRef] [PubMed]
34. Wang, R.; Chen, C.; Guo, S. Effects of drying methods on starch crystallinity of gelatinized foxtail millet (α-millet) and its eating quality. *J. Food Eng.* **2017**, *207*, 81–89. [CrossRef]
35. Chen, X.; Li, X.; Mao, X.; Huang, H.; Wang, T.; Qu, Z.; Miao, J.; Gao, W. Effects of drying processes on starch-related physico-chemical properties, bioactive components and antioxidant properties of yam flours. *Food Chem.* **2017**, *224*, 224–232. [CrossRef] [PubMed]
36. Fan, D.; Ma, W.; Wang, L.; Huang, J.; Zhao, J.; Zhang, H.; Chen, W. Determination of structural changes in microwaved rice starch using Fourier transform infrared and Raman spectroscopy. *Starch Stärke* **2012**, *64*, 598–606. [CrossRef]

37. Zhang, J.; Chen, F.; Liu, F.; Wang, Z.W. Study on structural changes of microwave heat-moisture treated resistant Canna edulis Ker starch during digestion in vitro. *Food Hydrocoll.* **2010**, *24*, 27–34. [CrossRef]
38. Olsson, A.M.; Salmén, L. The association of water to cellulose and hemicellulose in paper examined by FTIR spectroscopy. *Carbohydr. Res.* **2004**, *339*, 813–818. [CrossRef]
39. Kačuráková, M.; Mathlouthi, M. FTIR and laser-Raman spectra of oligosaccharides in water: Characterization of the glycosidic bond. *Carbohydr. Res.* **1996**, *284*, 145–157. [CrossRef]
40. Cael, J.J.; Gardner, K.H.; Koenig, J.L.; Blackwell, J. Infrared and Raman spectroscopy of carbohydrates. Paper V. Normal coordinate analysis of cellulose I. *J. Chem. Phys.* **1975**, *62*, 1145–1153. [CrossRef]
41. Siemion, P.; Jabłońska, J.; Kapuśniak, J.; Kozioł, J.J. Solid State Reactions of Potato Starch with Urea and Biuret. *J. Polym. Environ.* **2004**, *12*, 247–255. [CrossRef]
42. Kizil, R.; Irudayaraj, J.; Seetharaman, K. Characterization of irradiated starches by using FT-Raman and FTIR spectroscopy. *J. Agric. Food Chem.* **2002**, *50*, 3912–3918. [CrossRef] [PubMed]
43. Baianu, I.C.; Yakubu, P.I.; Ozu, E. Structural and hydration studies of waxy and mealy potato starch cultivars by deuterium, carbon-13 CP-MAS/MASS NMR, and electron microscopy. *Macromol. Symp.* **1999**, *140*, 187–195. [CrossRef]
44. Richardson, S.J.; Baianu, I.C.; Steinberg, M.P. Mobility of Water in Corn Starch Suspensions Determined by Nuclear Magnetic Resonance. *Starch Stärke* **1987**, *39*, 79–83. [CrossRef]
45. Hoover, R. Composition, molecular structure, and physicochemical properties of tuber and root starches: A review. *Carbohydr. Polym.* **2001**, *45*, 253–267. [CrossRef]
46. Liu, H.; Xie, F.; Yu, L.; Chen, L.; Li, L. Thermal processing of starch-based polymers. *Prog. Polym. Sci.* **2009**, *34*, 1348–1368. [CrossRef]
47. Zobel, H.F. Starch Crystal Transformations and Their Industrial Importance. *Starch Stärke* **1988**, *40*, 1–7. [CrossRef]
48. Jane, J. Structure of Starch Granules. *J. Appl. Glycosci.* **2007**, *54*, 31–36. [CrossRef]
49. Bogracheva, T.Y.; Morris, V.J.; Ring, S.G.; Hedley, C.L. The granular structure of C-type pea starch and its role in gelatinization. *Biopolymers* **1998**, *45*, 323–332. [CrossRef]
50. Srikanlaya, C.; Therdthai, N.; Ritthiruangdej, P.; Zhou, W. Effect of butter content and baking condition on characteristics of the gluten-free dough and bread. *Int. J. Food Sci. Technol.* **2017**, *52*, 1904–1913. [CrossRef]
51. Wang, L.; Wang, M.; Zhou, Y.; Wu, Y.; Ouyang, J. Influence of ultrasound and microwave treatments on the structural and thermal properties of normal maize starch and potato starch: A comparative study. *Food Chem.* **2022**, *377*, 131990. [CrossRef]
52. Dome, K.; Podgorbunskikh, E.; Bychkov, A.; Lomovsky, O. Changes in the crystallinity degree of starch having different types of crystal structure after mechanical pretreatment. *Polymers* **2020**, *12*, 641. [CrossRef] [PubMed]
53. Han, Z.; Li, Y.; Luo, D.H.; Zhao, Q.; Cheng, J.H.; Wang, J.H. Structural variations of rice starch affected by constant power microwave treatment. *Food Chem.* **2021**, *359*, 129887. [CrossRef] [PubMed]
54. Capron, I.; Robert, P.; Colonna, P.; Brogly, M.; Planchot, V. Starch in rubbery and glassy states by FTIR spectroscopy. *Carbohydr. Polym.* **2007**, *68*, 249–259. [CrossRef]
55. Chen, X.; Mao, X.; Jiang, Q.; Wang, T.; Li, X.; Gao, W. Study on the physicochemical properties and in vitro digestibility of starch from yam with different drying methods. *Int. J. Food Sci. Technol.* **2016**, *51*, 1787–1792. [CrossRef]